Geomagnetopause Position and Shape Dependence on Solar Wind Plasma and IMF Parameters: Analytic Model Comparison with Observations and 3-D MHD Runs

M. I. Verigin, G. A. Kotova and V. V. Bezrukikh

Space Research Institute of Russian Academy of Sciences, Profsoyuznaya, 84/32, Moscow, 117997, Russia, email: verigin@iki.rssi.ru

Abstract. It is generally accepted to use the solar wind ram pressure ρV^2 and the IMF B_z component for empirical description of the geo-magnetopause position and shape. A specific feature of the present paper is not to use the solar wind ρV^2 but the thermal P_{th} and magnetic field P_{mag} pressures adjacent to the magnetopause for proper modelling. These pressures are deduced from the results of 3-D MHD runs and analytic solutions for post bow shock MHD flow in Lagrangian variables. The magnetopause shape variation due to B_z component changes the so called 'doubling factor' f_d, which can be analytically deduced from a Tsyganenko magnetospheric field ellipsoidal model. Including all the above effects in our analytical model leads to a good description of 'rapid' magnetopause approach to the Earth for southward IMF and to its 'stagnant' behaviour with the increase of northward IMF component.

Keywords. Magnetopause, solar wind ram pressure, magnetic and thermal pressure, doubling factor

1. Introduction

It is generally accepted that the solar wind ram pressure ρV^2 is the main factor contributing to the magnetopause stagnation pressure, which can be then approximated as $\Pi \approx k\rho V^2$ with k being a function of solar wind specific heat ratio γ and sonic Mach number M_s (Landau & Lifshits 1959):

$$k = \frac{1}{\gamma}\left(\frac{\gamma+1}{2}\right)^{(\gamma+1)/(\gamma-1)}\left(\gamma - \frac{\gamma-1}{2M_s^2}\right)^{1/(1-\gamma)}. \tag{1}$$

Complementary factors that are influencing the magnetopause position and shape are: (i) the magnetic field tension resulting in the clock angle dependency of the magnetopause terminator cross-section (Verigin *et al.* 2009), (ii) the magnetic field pressure leading to magnetopause movement towards the Earth when the IMF cone angle approaches $\pi/2$ (Dušík *et al.* 2010), and (iii) the IMF B_z component increasing the magnetopause nose bluntness for southward B_z direction (Sibeck *et al.* 1991). It was shown (Verigin *et al.* 2014) that the contribution of the magnetic field tension to the stagnation pressure is $2\Delta/R$ times less than contribution of the magnetic pressure itself, where Δ is the magnetosheath thickness and R is the magnetic field lines curvature radius. Thus tension effects will be omitted in subsequent analysis.

The following expression presents one of the widely used relations for magnetopause shape description (see, e.g., Liu *et al.* 2015):

$$r = r_0 \cdot \left(\frac{2}{1+\cos\theta}\right)^{\alpha} \cdot \left(1 - 0.1 \cdot C\cos^2\phi\right), \tag{2}$$

121

where r_o is the planetocentric distance to the magnetopause nose position, θ and φ are the polar and azimuth angles, respectively; the second multiplier is the global magnetopause shape factor, while the third multiplier describes the local cusps depression and will not be considered further. Flaring angle α and r_0 in the relation (2) are *empirical* functions incorporating physically unjustified *multiplicative* function of IMF B_z component, and power function of a *simple sum* of solar wind ram and magnetic pressures.

It seems apparent that using, not the solar wind ram pressure, but the thermal, magnetic and total pressures adjacent to the magnetopause, and better justified magnetopause shape variation with B_z are preferred for the magnetopause position and shape modeling, and it is this approach which will be used further.

2. Basic approach and relations

Empirical relations for the description of the total P_{tot}, thermal P_{th}, and magnetic field P_{mag} pressures at the magnetopause nose are based on the results of 3-D MHD modelling (Stahara 2002) and analytic solutions in Lagrangian variables (Shugaev *et al.* 2005). For the case of interplanetary magnetic field perpendicular to the solar wind velocity (Verigin *et al.* 2015):

$$P_{tot} = k\rho V^2 (1 + (\sqrt{6}\big/ M_a^2)^{2/3}), \tag{3}$$

$$P_{th} = k\rho V^2 /(1 + 25 \cdot (2 - \sqrt{6/M_s})/M_a), \tag{4}$$

$$P_{mag} = \Pi - P_{th}, \tag{5}$$

where M_a is the Alfvénic Mach number. Figure 1 shows the pressures defined in (3 - 5) as functions of $1/M_a$ and the good correspondence with results of 3-D MHD modelling (Stahara 2002).

The following important relation of our approach describes a so-called 'doubling factor' f_d, which indicates how much the internal magnetospheric field is increasing in the subsolar region due to Chapman-Ferraro currents. Using the ellipsoidal model of Tsyganenko (1989) we approximated f_d by the following relation :

$$f_d(r_0/R_0) = (4 + 5r_0/R_0)/3, \tag{6}$$

where R_o is the magnetopause nose curvature radius. Figure 2 demonstrates the good correspondence of relation (6) with the results of the model (Tsyganenko 1989). According to (6) frequently used in modeling, the doubling factor $f_d \approx 2.44$ (see, e.g., Beard 1964) corresponds to reasonable magnetopause nose shape with $R_o \approx 1.5\ r_o$ (Verigin *et al.* 2009).

Relation (6) corresponds to the theoretical case with $\boldsymbol{B}_{IMF} = 0$. The presence of non-zero $\boldsymbol{B}_{IMF}$ in the solar wind flow will lead both to r_o and R_o variations: $r_o \to r_b$ and $R_o \to R_b$. We estimated new ratio of $r_b\ /\ R_b$ as:

$$r_b/R_b = (1 \pm \xi\sqrt{P_{mag}/P_{tot}}) \cdot r_0/R_0, \tag{7}$$

where ξ is yet an undefined parameter describing the variation of magnetic field in the magnetosphere adjacent to the magnetopause due to external non-zero magnetosheath field $\sqrt{8\pi P_{mag}}$, and +/- signs correspond to northward and southward IMF directions, respectively. The pressure balance equation for the northward IMF case can be written as:

$$B_e \cdot (R_e/r_{b+})^3 \cdot (f_d(r_0/R_0) + \xi \cdot 5r_0/3R_0 \cdot \sqrt{P_{mag}/P_{tot}}) = \sqrt{8\pi P_{tot}}, \tag{8}$$
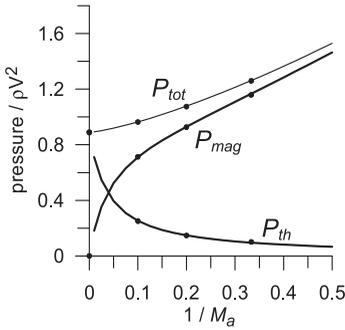
Figure 1. Comparison of 3-D MHD calculations (dots) with approximating relations (3 - 5).
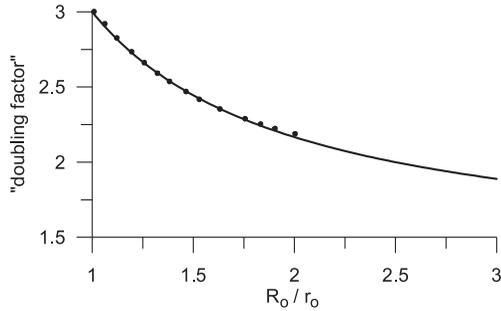
Figure 2. Comparison of Tsyganenko (1989) model results (dots) with calculations by the expression (6).
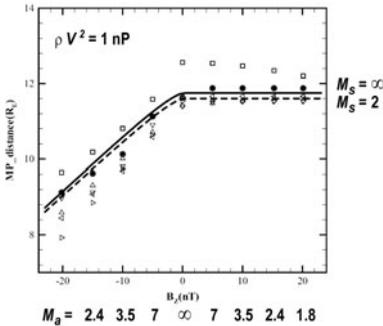
Figure 3. Comparison of the present analytic model (solid and dashed lines lines) with the modern 3-D MHD modeling results (●-, Lu *et al.* 2015) and with widely used empiric models: upward triangles (Shue *et al.* 1997), downward triangles (Shue *et al.* 1998), left triangles (Petrinec & Russell 1996), right triangles (Chao *et al.* 2002), squares (Lin *et al.* 2010).

where $B_e = 31{,}200$ nT, $R_e = 6{,}371$ km. Due to the "stagnant" position of the magnetopause under northward IMF: $r_{b+} \approx r_o$. Taking into account that $B_e \cdot (R_e/r_0)^3 \cdot f_d(r_0/R_0) = \sqrt{8\pi k\rho V^2}$ we can deduce the ξ factor as:

$$\xi = \sqrt{P_{tot}/P_{mag}} \cdot (\sqrt{P_{tot}/k\rho V^2} - 1) \cdot (1 + 4R_0/5r_0). \tag{9}$$

Subsequent substitution of the expression for ξ (9) into equation similar to (8), but with negative sign before ξ and $r_{b+} \to r_{b-}$, will lead to evaluation of the magnetopause nose position r_{b-} for southward IMF direction:

$$r_{b-} = r_0 \cdot \sqrt[3]{2 \cdot \sqrt{k\rho V^2/P_{tot}} - 1}. \tag{10}$$

The magnetopause nose curvature radii for northward and southward IMF direction R_{b+}, R_{b-} can now be calculated with the use of relation (7) with proper sign. It demonstrates the increase of the ratio R_b/r_b with the increase of southward IMF B_z component that provides more blunt magnetosphere nose in this case, and decrease of the ratio R_b/r_b with increase of northward IMF B_z component that provides 'sharpening' of the magnetopause nose for the northward IMF.

Figure 3 presents comparison of the present analytic model of the magnetopause nose position variation with IMF B_z component (for $M_s = 2$ – dashed line and for $M_s \to \infty$ - solid line), with the results of bulky 3-D MHD modeling by Lu *et al.* (2015). A good correspondence can be observed. Note that though condition $r_o = const$ for $B_z > 0$ was implemented in the model, coincidence of the slopes of the both modeling curves for $B_z < 0$ provides evidence of the validity of our analytic modeling approach.

3. Summary and Conclusions

Including theoretically derived relations (3 - 7) into a magnetopause model (see also Verigin *et al.* 2009, 2015) makes it possible to describe a variation of the magnetopause position and shape for a wide range of solar wind ram pressures and IMF B_z components.

Qualitatively, an increase in either northward or southward IMF B_z component leads to an increase of the total magnetosheath pressure at the stagnation point (see relation (3)) thus suggesting magnetopause motion toward the planet. On the other hand, the dependence of the magnetopause shape R_b/r_b (7) and 'doubling factor' (6) on IMF B_z component provides "blunted" magnetopause for southward IMF and "sharpened" magnetopause for northward IMF. Decreased 'doubling factor' (6) for southward IMF leads to a relatively "rapid" approach of "blunted" magnetopause toward the Earth while increased f_d for northward IMF provides "stagnant" behavior of the "sharpened" magnetopause, that qualitatively corresponds to magnetopause observations (see, e.g., Sibeck *et al.* 1991).

References

Beard, D. B., 1964, *Rev. Geophys.* 2(2), 335

Chao, J. K., Wu, D. J., Lin, C.-H., Yang, Y. H., Wang, X. Y., Kessel, M., Chen, S. H. & Lepping, R. P. 2002, in: L.-H. Lyu (eds.), *Space weather study using multipoint techniques*, *COSPAR Colloq. Ser.*, (Pergamon: Oxford), v.12, p.127

Dušík, Š., Granko, G., Šafránková, J., Němeček, Z. & Jelínek, K. 2010, *Geophys. Res. Lett.*, 37, L19103, doi:10.1029/2010GL044965

Landau, L. D. & Lifshitz, E. M. 1959, *Fluid Mechanics*, (Pergamon Press: London)

Lin, R. L., Zhang, X. X., Liu, S. Q., Wang, Y. L. & Gong, J. C. 2010, *J. Geophys. Res.*, 115, A04207. https://doi.org/10.1029/2009JA014235

Liu, Z.-Q., Lu J. Y., Wang C., Kabin K., Zhao J. S., Wang M., Han J. P., Wang J. Y. & Zhao M. X. 2015, *J. Geophys. Res. Space Physics*, 120, 5645, doi:10.1002/2014JA020961

Lu, J. Y., Wang, M., Kabin K., Zhao J. S., Liu Z.-Q., Zhao M. X. & Li, G. 2015, *Planetary and Space Science*, 106(2), 108

Petrinec, S. M. & Russell, C. T. 1996, *J. Geophys. Res.*, 101(A1), 137

Sibeck, D. G., Lopez, R.E & Roelof, R. C. 1991, *J. Geophys. Res.*, 96(A4), 5489

Shue, J.-H., Chao, J. K., Fu, H. C., Russell, C. T., Song, P., Khurana, K. K. & Singer, H. J. 1997, *J. Geophys. Res.*, 102(A5), 9497. https://doi.org/10.1029/97JA00196

Shue, J.-H., Song, P., Russell, C. T., Steinberg, J T., Chao, J. K., Zastenker, G., Vaisberg, O. L., Kokubun, S., Singer, H. J., Detman, T. R. & Kawano, H. 1998, *J. Geophys. Res.* 103(A8), 17691. https://doi.org/10.1029/98JA01103

Shugaev, F. V. & Kalinchenko A. P. 2005, in: V. A. Bityurin (ed.) *Proceedings of the 15 International Conference on MHD Energy Conversion and the 6 International Workshop on Magnetoplasma Aerodynamics*, (IVTAN: Moscow), v.2, p.617

Stahara, S. S. 2002, *Planet. and Space Sci.*, 50, 421

Tsyganenko, N. A. 1989, *Planet. and Space Sci.*, 37(9), 1037

Verigin, M. I., Kotova, G. A., Bezrukikh, V. V., Zastenker, G. N. & Nikolaeva, N. F. 2009, *Geomagn. and Aeronomy*, 49(8), 1176

Verigin, M., Tatrallyay, M., Erdos, G., Kotova, G., Bezrukikh, V. & Remizov, A. 2014, *The 40-th COSPAR Scientific Assembly*, 2–10 Aug. 2014, Moscow, Russia, Abstract D3.5-0014-14, 2014

Verigin, M. I., Kotova, G. A., Bezrukikh, V. V. & Remizov A. P. 2015, *EPSC Abstracts*, v. 10, EPSC2015-708